Contract No:

This document was prepared in conjunction with work accomplished under Contract No. DE-AC09-08SR22470 with the U.S. Department of Energy (DOE) Office of Environmental Management (EM).

Disclaimer:

Proceedings of the ASME 2017 Pressure Vessels & Piping Conference
PVP2017
July 16-20, 2017, Waikoloa, Hawaii, United States

PVP2017-66105

CRACK GROWTH RATE TESTING WITH INSTRUMENTED BOLT-LOAD COMPACT TENSION SPECIMENS UNDER CHLORIDE-INDUCED STRESS CORROSION CRACKING CONDITIONS IN SPENT NUCLEAR FUEL CANISTERS

Andrew J. Duncan
Materials Science and Technology
Savannah River National Laboratory
Aiken, SC 29808, USA
andrew.duncan@srnl.doe.gov

Poh-Sang Lam
Materials Science and Technology
Savannah River National Laboratory
Aiken, SC 29808, USA
ps.lam@srnl.doe.gov

Robert L. Sindelar
Materials Science and Technology
Savannah River National Laboratory
Aiken, SC 29808, USA
robert.sindelar@srnl.doe.gov

Joe T. Carter
Nuclear Programs
Savannah River National Laboratory
Aiken, SC 29808, USA
joe.carter@srs.gov

ABSTRACT

Stress corrosion cracking (SCC) may occur when chloride-bearing salts and/or dust deliquesce on the external surface of the spent nuclear fuel (SNF) canister at weld residual stress regions. An SCC growth rate test is developed using instrumented bolt-load compact tension specimens using the American Society for Testing Materials (ASTM) specification E1681 with an experimental apparatus that allows an initially dried salt to deliquesce and infuse naturally to the crack front under temperature and humidity parameters relevant to the canister storage environmental conditions. The shakedown tests were conducted over a range of relative humidity controlled by the guidance in ASTM E104 at 50 °C with salt assemblages of (1) mixture of artificial dust and deliquescent salts (2) a mixture of artificial dust and salt from dehydrated sea water. After five months exposure the specimens were examined for evidence of chloride induced stress corrosion cracking (CISCC) and observations are reported for both salt/dust mixtures. The test specimen and apparatus designs will be modified to enhance the interaction between the deliquescing salt and the crack front for more accurate characterization of the crack growth rate as a function of stress intensity factor, which is an essential input to the determination of in-service inspection frequency of SNF canisters.

INTRODUCTION

Dry cask storage systems are deployed throughout the world for storage of spent nuclear fuels. Dry shielded canister (DSC) designs include welded, austenitic stainless steel multipurpose canisters (MPC) that are placed within concrete overpacks and stored on an outside pad [1]. The overpacks are vented to the atmosphere to allow for cooling of the canister by convective air flow. Experimental studies have shown that stainless steels typical of those used for the canisters (e.g. 304, 304L, 316, or 316LN) are susceptible to stress corrosion cracking with chloride-containing salts [2-6]. Salts are transported in aerosol droplets from sea water and continental sources on air currents and are entrapped in dust layers or deposited on the surfaces everywhere including MPCs [6]. Moist chloride-rich salt deposits are aggressive to stainless steel, particularly at weld heat-affected-zone (HAZ) regions with sensitized microstructures and residual stresses. Because heat treatment for stress relief is not required for the construction of MPCs, the canister is expected to retain residual stress (RS) from its fabrication and closure welds. These stresses have been directly measured [7] and estimated [1] using recommendations from API-579 [8]. These studies show that the canisters sections adjacent to weldments can retain RS in excess of the yield strength of the base metal. Hence, it is possible for canisters to be susceptible to CISCC in the weld or HAZ regions under long-term storage conditions. A potential degradation scenario has been identified which involves chloride-rich salts being deposited from air onto the canisters through atmospheric convection,

over time. If the local relative humidity at the canister surface is high enough, salts may deliquesce and form aggressive brine that may undermine the integrity of canisters [4].

No evidence of pitting or CISCC on canisters due to corrosion has been observed to date. Nevertheless, the U.S. Nuclear Regulatory Commission is requiring the dry storage licensees to institute an Aging Management Program (AMP) to demonstrate that the structural integrity and confinement function of the canisters is maintained for extended (re-license) storage conditions in consideration of the potential for SCC [9]. Consensus rules for in-service inspection of the canisters are being developed, and these rules can serve as the foundation for the canister AMP and a Task Group was constituted in 2015 to provide a new code case for the American Society of Mechanical Engineers (ASME) Boiler and Pressure Vessel Code under Section XI [10].

Flaw acceptance criteria for the disposition of the inspection results will be needed if relevant indications are found during the examination. Disposition of flaws that would be identified as stress corrosion cracks, and characterized or sized using visual, surface, and volumetric examination methods. Inputs to the technical bases will include the evaluation of flaw stability under design basis loading cases, and also allowance for flaw growth between inspection intervals.

For stainless steels, it is commonly concluded that canisters are highly tolerant of flaws. However, when residual stress is included as part of the loading in the analysis and if consideration is given to elastic-plastic fracture mechanics through the Failure Assessment Diagram (FAD) formulation [8], the instability crack sizes are significantly reduced from those based on the net section yielding limit load failure criterion and more conventional code based analyses [1, 12]. Hence, accurate and reliable crack growth velocities become of increasing importance for reliable flaw disposition.

The challenge with generating data relevant and directly applicable to the DSC is the environmental loading and testing for what is called “dry salt” conditions. That is, with initial fully dried deposits on the canister surface, and under falling canister temperatures with extended times, the deposits with deliquescing salts will eventually create the aggressive environments but at an uncertain rate and severity.

CRACK GROWTH KINETICS

Crack Growth Rate (CGR) testing aimed at conditions for a DSC in natural exposure settings and with salt assemblages loaded onto the specimens has been performed over the past several years. Researchers at Central Research Institute of Electric Power Industry (CRIEPI) in Japan have generated the largest data sets to date [13-16]. The specimen designs included 4-point bend [4], 3-point bend [14, 15], and compact tension (CT) [13, 16]. Figures 1 and 2 show the specimen designs, mechanical loading and the corresponding crack growth rates measured for these tests. The wide range of CGR (0.5-32 mm/yr) is evident from these figures. The impact of these rates on the disposition of flaws and proposed inspection frequency would be difficult to implement without further understanding the role of environment and service conditions on CGR.

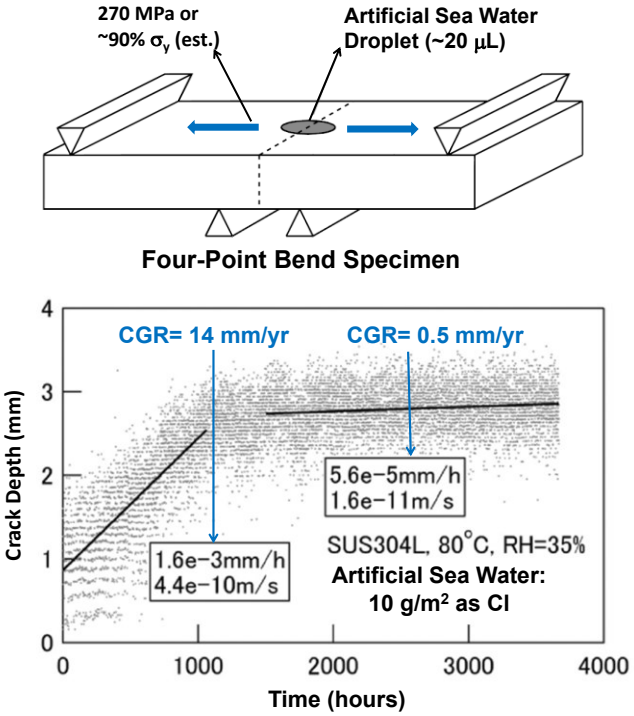

FIGURE 1: 4-POINT BEND TEST SPECIMEN CONFIGURATION AND RESULTS - reproduced from reference [4] - (the specimen may not have contained a pre-crack)

It is not clear if cracking was initiated prior to the test and the flaw configuration was not controlled, which could complicate estimating stress intensity factors (K) at the crack tip. Specimens can be tested without pre-cracks, however pre-cracks are typically used to provide a defined initial crack front in a specimen. Fatigue pre-cracking in air was used in the testing with 3-point bend and Compact Tension (CT) design specimens in the CRIEPI testing [13-16]. The aggressive environmental conditions used to load the crack growth test specimens was chloride solutions or artificial seawater. Natural exposure testing was also used in the 3-point bend specimen testing.

Phenomenologically, CGR typically is dependent on the applied K (applied to crack tip). A threshold stress intensity, K_{ISCC}, can be observed, below which SCC does not propagate. At higher K, a region of K dependency exists. Finally, rapid increase in CGR is observed until fast fracture occurs at K levels approaching the materials fracture toughness. From Figures 1 and 2, there appears to be insensitive between K and crack growth rate.

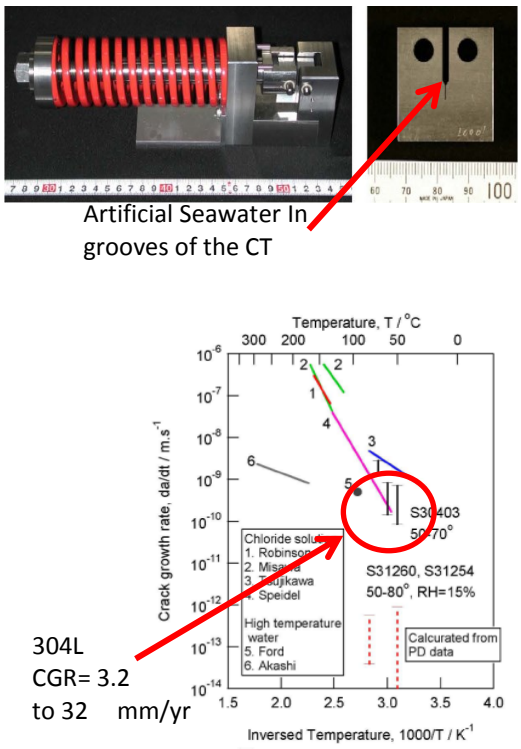

FIGURE 2: CT TEST SPECIMEN CONSTANT LOAD CONFIGURATION AND RESULTS – reproduced from reference [13]

Results vary widely among the available literature on CGR testing under conditions similar to the deliquescent salt conditions on the canister. This appears to be due, in part, to the difficultly in crack nucleation, the crack establishing a uniform crack front with sufficient electrolyte and of relevant salt brine composition. Previously, a new "dry salt" SCC specimen test configuration was designed to overcome the stochastic nature of crack nucleation and the irregular crack front during propagation [17]. The test specimen was pre-cracked in fatigue with side grooves and a holder to maintain intimate contact between the specimen and the dry salt used to simulate chloride bearing deposits. The loading configuration affords the real time measurement of load vs time by which crack growth rate can be determined. Further, the configuration would allow the characterization of the K dependency in a single test setup. In the current study, preliminary results of a testing demonstration are presented. The method did not successfully demonstrate real time crack growth measurement but does reveal useful information of CISCC in the current system.

EXPERIMENTAL DRY SALT CRACK GROWTH TESTS: LOADING AND OPERATION

Experiments were conducted on type 304 stainless steel. Conditions were selected to simulate service conditions for the dry storage canisters. Figure 3 shows the sketch of the dry salt SCC test configuration concept that uses a Bolt Loaded Compact Tension (BLCT) specimen per ASTM E1681 [18] that is loaded with an instrumented bolt. The assemblage contains a special cradle to hold a salt mixture against the external faces of the specimen. Such a configuration allows the conditions favorable for stress corrosion cracking to occur in a manner similar to service conditions (i.e., salt to deliquesce naturally from water vapor in the environment and wick into the notch).

The stress intensity factor, K, is determined for the crack front per the equation 4 of ASTM E1681 standard and is dependent on crack length, a, specimen compliance, Young's Modulus, E, Crack mouth Opening Displacement (COD) and the specimen width, W. Unlike service conditions the SCC testing is conducted under "falling K" kinetics that would allow for the examination of the relationship between K and crack growth rate, as well as, provide data to determine a threshold value for stress corrosion cracking, if one exists (see Figure 4). The arrows in the graph illustrate the relationship between K and a/w[1] for a COD values used in this study. As the crack grows, K drops until the CGR also stops. This is referred to as K_{ISCC}.

The specimen design was selected with consideration of constraint based fracture mechanics. Since the dimensions that would enable plane strain conditions in the specimen design with austenitic stainless steel are not met, the derived K is termed K_{JC} to reflect that plasticity conditions exist at the crack tip in the testing. Pre-cracks were initiated in the specimens by fatigue in air to intermediate ratio of crack length/ specimen width (a/w ≅ 0.50-0.65). Fatigue cracking was conducted at stress intensity factors as low as possible consistent with developing a crack in the specimens within 24 hours. The specimens were cleaned in isopropanol and dried. The cleaned specimens were then loaded to desired stress intensity factors. This was achieved by first elastically loading and unloading specimens in an Instron 4507 mechanical testing machine while recording load and COD. The specimens were then reloaded in a vice with an instrumented bolt to a critical COD value corresponding to the desired stress intensity factor. Specimens were loaded in a cradle with the desired dry salt/dust mixture and placed in controlled humidity chamber. The cradle was machined from a porous frit, and its porosity allows a humid air contact to the salt mixture.

Figure 5 shows the actual test assembly used during testing. The glass vessel shown contains saturated brine at the bottom of the vessel to control the Relative Humidity (RH) in accordance with ASTM E104 [19]. The vessel is placed in an oven for temperature control. Atmospheric conditions are monitored using a Vaisala HUMICAP® Hand-Held Humidity and Temperature Meter HM70 equipped with a high temperature probe tip. The feed-through on both the glass vessel and the oven enable a Data Acquisition System (DAS) to acquire load drop with time for a fixed displacement (COD).

Three conditions were tested and are summarized in Table 1. The dust/salt constituents are a mixture of CeO_2 + 2%

[1] a/w ≡ crack length/specimen width (see figure 3)

mixture of NaCl/KCl/$CaCl_2$ (Specimen 1) and a mixture of simulated inorganic dust and artificial sea salt (Specimens 2 and 3). The temperature and humidity conditions were selected. to bound ambient conditions and were held constant at 50 ºC. Constant relative humidity levels of 30% (Specimen 3) and 50% (Specimen 1 and 2) were maintained at all times for the duration of testing. The salt composition for Specimen 1 were chosen based on previous corrosion studies [20] as an artificially aggressive condition because of the high level of $CaCl_2$. The atmospheric conditions of Specimens 1 and 2 were chosen to be artificially aggressive (50% RH) while Specimen 3 at 30% RH was selected based on its relevance to the upper bound of expected service conditions of the DSC [6].

Additional specimens were inserted next to the specimens in each vessel (see Figure 5). Teardrop specimens made from 304L were held in glass cradles and utilized to gather visual evidence of the deliquescence and/or corrosion of specimens without unloading the BLCT and removing them from the environment. The specimens were exposed to the same experimental conditions for 5 months and examined.

EXPERIMENTAL DRY SALT CRACK GROWTH TESTS: CHARACTERIZATION AND ANALYSIS

Using the instrumented bolts, algorithms can be applied to estimate the crack length and applied K real time. However, in-situ data was not used to determine final K. This is due in part because the instrumented bolts experienced some drift during the testing period. Removing the cumulative effects of this drift made calibrating the signal difficult. Instead, specimens were removed from the vessel and cleaned in de-ionized water followed with rinsing in isopropanol and dried. Figure 6 shows the specimens as they were removed from the test vessel. Crack lengths were examined after exposure using an optical microscope on both sides of the specimen surfaces. The measured crack lengths were compared to the initial values measured for each specimen.

The specimen compliance and final load on the specimen were determined by unloading the specimen and reloading in the Instron while recording load and crack opening-displacement (COD). These values were compared to initial results. The specimens were then heat tinted 350°C for 30 minutes and fatigued until the crack grew to the back face of the specimen. The final crack length was measured under an optical microscope in accordance ASTM E1681 at the transition from heat tint and un-oxidized fatigue surface. The fracture surface was characterized using an Scanning Electron Microscope (SEM) equipped with an Energy Dispersive Spectrometer (EDS) for elemental analysis.

EXPERIMENTAL RESULTS

The specimens were removed after 5 months at of exposure. Figure 6 illustrates the appearance of the specimens after exposure. Both the BLCT and Teardrop specimens in Test cell 1 exhibited corrosion around where the specimen made contact with dust. They also had the dust/salt mixture clumped on their surfaces. Figure 7 shows the type of corrosion visible on the teardrop from Test cell 1. The BLCT and Teardrop specimens in Test cells 2 and 3 did not and have any visible corrosion and had a smaller amount of dust adherent to surfaces.

The final crack lengths were measured in three ways. First, the crack were measured in each side groove and averaged. However, the crack length in specimen 1 could not be visually measured in the side groove because the crack front was obscured by corrosion. Next, compliance for each specimen was measured using the Instron test machine and a COD clip gage in Specimens 1-3. The results are captured in Table 2. The specimen compliance appeared to be unchanged from the pretest measurement. Finally, the specimens were heat tinted to mark the crack front and fatigued open. Images of fracture surfaces from specimens 1-3 are presented in Figures 8-10, respectively. Specimen 1 showed evidence of a large crack on the fracture surface (see Figure 8). The crack appears to have nucleated from the edge of the side groove and grown inward toward the center. Unfortunately, this crack was not planar or straight. This makes estimating the K at the crack front using equation 4 of ASTM E1681 impossible. Specimens 2 and 3 show no significant crack growth after 5 months (see Figures 9 and 10).

DISCUSSION

From the results presented in Figures 7-10, it is apparent that Test 1 dust/salt mixture is more aggressive than Tests 2 and 3. The presence of pitting in the teardrop (Figure 7) and BLCT fracture surface (Figure 8) help illustrate that point. In addition, the cracking in Specimen 1 also shows the difficulties in measuring CGRs of this nature with the test setup. Given enough time and moisture, the crack should have continued to grow at a rate that was dependent on the falling K until K_{ISCC} was reached. However, the crack continued to grow but not in planar manner or straight line. The cracking was transgranular accompanied with several secondary cracks propagating above and below the primary plane. If the crack originating from the side groove in Specimen 1 had a planar configuration, which would enable its proper characterization, the CGR of this sample would have exceeded 1 mm/year. These rates are not inconsistent with previous studies. Evidence of Cl^- salt deposits and pits were observed by EDS at the crack front and in secondary cracks adjacent to the crack plane. The side grooved region of the surface also exhibited pitting with secondary cracks emanating from them. Although the results have limited application for DSC's operating conditions, the results are consistent with previous data from calcined salt residues [20].

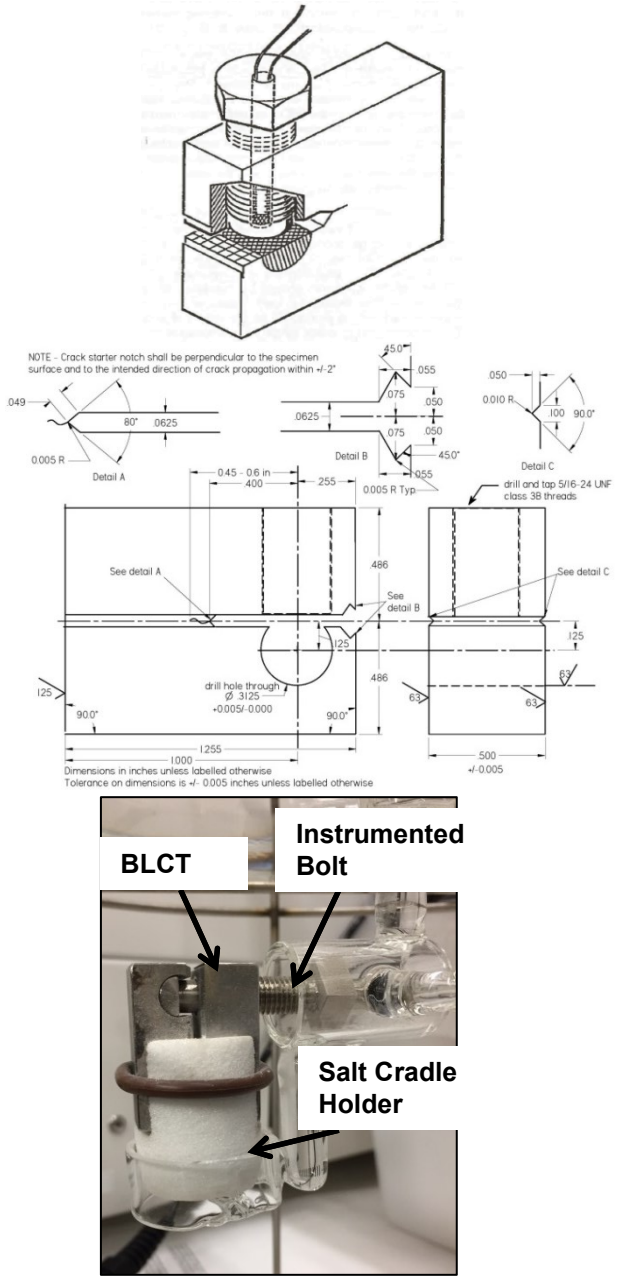

FIGURE 3: ASTM E1681 BOLT-LOADED COMPACT TENSION SPECIMEN DESIGN, 20% SIDE-GROOVED, IN A SALT CRADLE & AN INSTRUMENTED BOLT

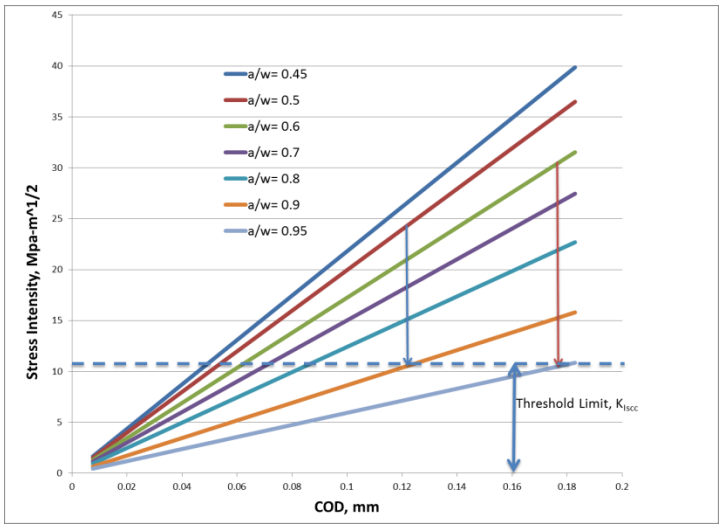

FIGURE 4: EXPECTED CRACK GROWTH BEHAVIOR OF "FALLING K" CONSTANT DISPLACEMENT TEST

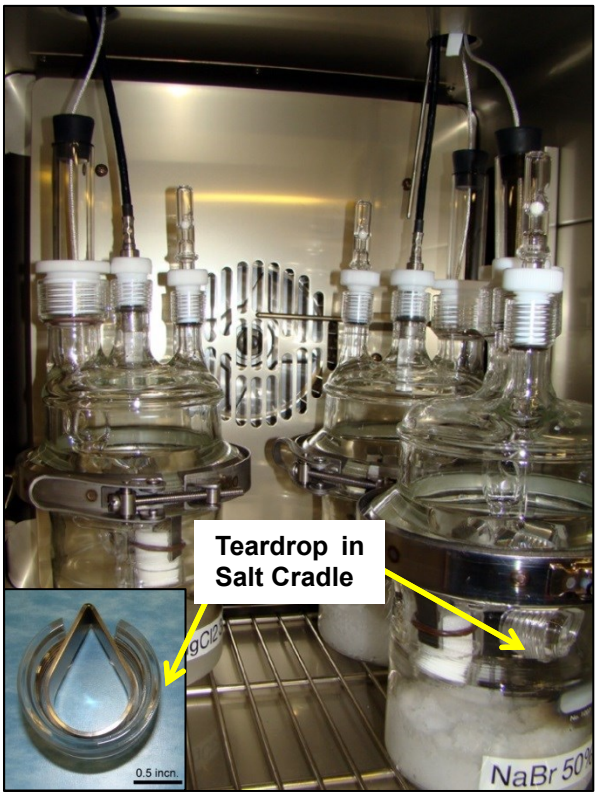

FIGURE 5: SCC TEST CONFIGURATION SHOWING THE CRADLED BLCT WITH AN INSTRUMENTED BOLT AND A COMPANION TEARDROP COUPON IN A CONSTANT HUMIDITY VESSEL

TABLE 1: EXPERIMENTAL CONDITIONS OF EXPOSURE IN DRY SALT CRACK GROWTH TESTING

Test	Environmental Conditions	Simulated Dust	Initial Crack Length (a/w)	Stress Intensity Factor (MPa-√m)
1	50 ºC 50 %RH†	98% CeO_2 0.8% NaCl 0.8% KCl 0.4% $CaCl_2$	0.55	32
2	50 ºC 50 %RH†	50% Washed Sand* 25% artificial sea salt$ 12.5% Kaolin 12.5% Feldspar	0.59	31
3	50 ºC 30 %RH‡	50% Washed Sand* 25% artificial sea salt$ 12.5% Kaolin 12.5% Feldspar	0.49	26

* Secondary components of Quartz sand can be Zircon, Ilmenite and Rutile
† Achieved using ASTM E104 saturated aqueous solution of NaBr
‡ Achieved using ASTM E104 saturated aqueous solution of $MgCl_2$
$ Dehydrated from artificial sea water of composition and form specified by ASTM D 1142

FIGURE 6: SPECIMENS AS THEY WERE REMOVED FROM TEST CELL (Cell 1: calcined salt, Cell 2 Sea Salt)

FIGURE 7: PITS ON SURFACE OF TEARDROP SPECIMEN IN TEST CELL 1 EXPOSED AFTER CLEANING (LOW MAG INSET)

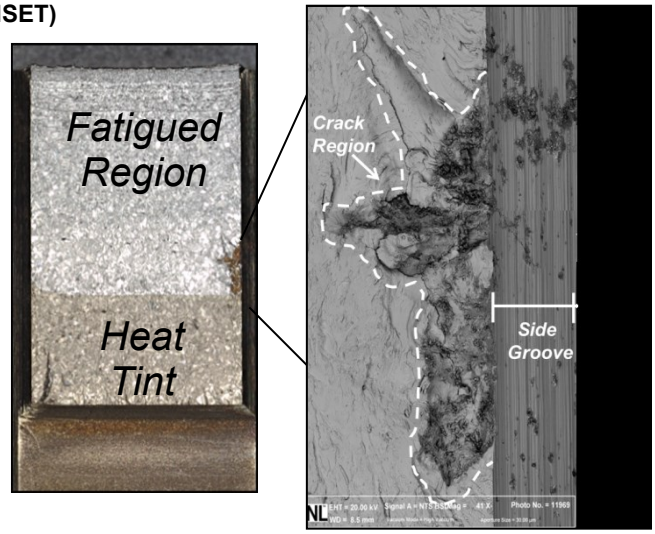

FIGURE 8: OPTICAL AND SEM IMAGES OF FRACTURE SURFACE OF SPECIMEN 1

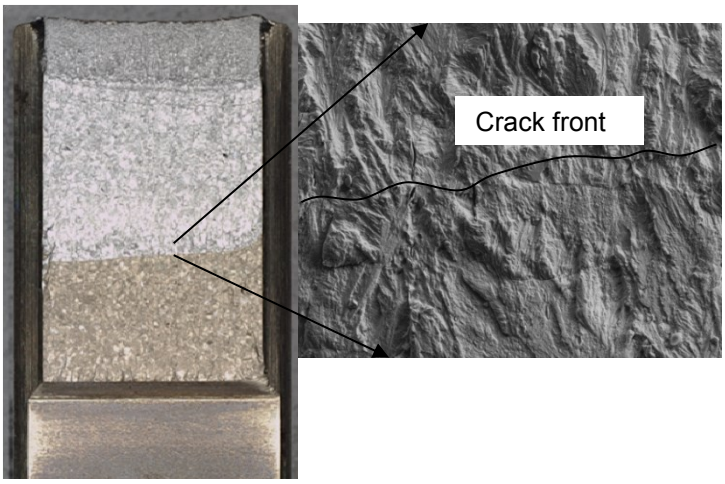

FIGURE 9: OPTICAL AND SEM IMAGES OF FRACTURE SURFACE OF SPECIMEN 2 (SEA SALT 50% RH)

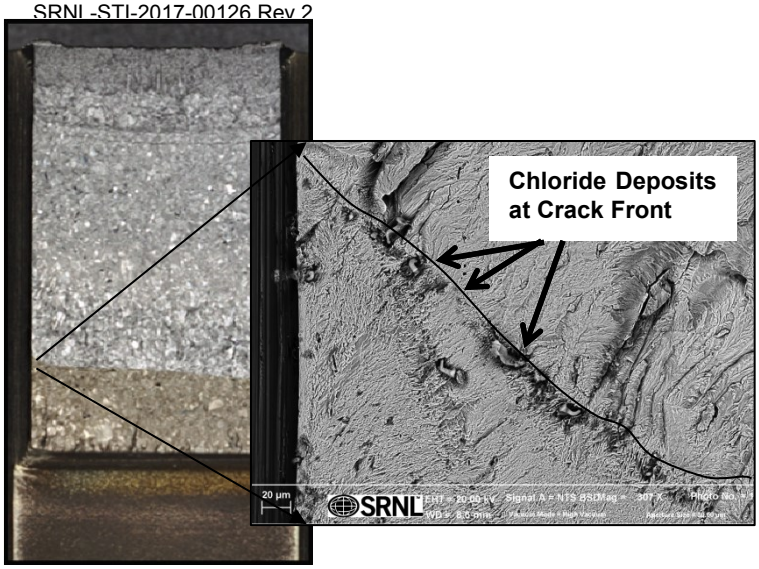

Figure 10: OPTICAL AND SEM IMAGES OF FRACTURE SURFACE OF SPECIMEN 3 (SEA SALT 30% RH)

TABLE 2: FINAL CRACK GROWTH DATA AS DETERMINED BY SPECIMEN COMPLIANCE

Test	Environmental Conditions	Initial Crack Length (a/w)	Stress Intensity Factor (MPa-√m)	Final Crack Length (a/w)
1	50 °C 50 %RH	0.55	32	0.55*
2	50 °C 50 %RH	0.59	31	0.59
3	50 °C 30 %RH	0.49	26	0.49

* Crack formation was observed by SEM examination of fracture surface in high stress intensity location (see Figure 8)

The results from Tests 2 and 3 are not as easy to interpret. Although the dust mixture was sand, feldspar, clay and artificial sea salt, the dust mixture did not adhere to the specimens as the calcined residues. The mixture appeared dry when removed from the Test cells 2 and 3, yet when baked in the oven at 105 °C the dust/salt mixture from Test cell 2 lost approximately 4 wt. % of its mass (presumably from moisture). No pitting was observed on the Teardrop or the BLCT specimens from Test 2 or 3. Secondary cracking associated with MnS inclusions (verified by EDS), was noted on the fatigue and fracture surfaces of the BLCT specimens. Some minor chloride containing deposits were observed at the pre-crack front on Specimen 3 (see deposits in Figure 10). One possible explanation for the absence of pitting/cracking is that the moisture content of the salt in Tests 2 and 3 may not be sufficient to provide the continuous film of electrolyte needed to promote corrosion under 30 or 50% RH conditions. If this is the case, the possibility for localized cracks or pits to form under isolated droplets of brine may still occur but would be expected to a lesser degree. Additionally, the direct, tight contact of the salt/dust mixture against the specimen is anticipated to be variable at a given local site. Coupled with deliquescence of the salt in the mixture, the resultant formation of brine to provide the electrolyte in contact with the specimen can be uncertain at any given site on the specimen for experimentation approach used in this investigation. Figure 6 is evidence that only local regions on the cell 1 specimens had a salt/dust mixture that had contact with the specimen and that formed brine sufficient to adhere the mixture to the specimen and promote corrosion.

Further teardrop testing was initiated to confirm the initial observations. After 3 additional months in Test cell 2 conditions (50 ºC, 50% RH), evidence of local pitting and/or cracking was observed in the Teardrop specimen. The difficultly in establishing conditions whereby the salt/dust mixture corrodes the stainless steel shows that such the mixtures, under moderate humidity conditions, may not always be sufficiently aggressive to attack the stainless steel. Further study is needed to elucidate the nature of this attack and the specimen(s) will be fully characterized and reported in the future.

CONCLUSIONS AND PATH FORWARD

Corrosion and stress corrosion cracking resistance was examined for stainless steels in dry salt environments. At the exposures in this study (50 °C and 50% RH), simulated calcined salt residues deliquesce to provide adequate electrolyte which leads to pitting corrosion and cracking in 304 stainless steel. The nature of the cracking was not planar and was difficult to characterize. In both sea salt tests that used artificial sea salt/dust mixtures, the corrosion or cracking was not present after 5 months. During a subsequent 3 months of exposure at these conditions pitting and cracking was observed in Teardrop specimens. This points to the fact that the conditions required for corrosion and cracking may require “significant” amounts of brine to accumulate on the surface of the specimens.

Future work on this topic includes the following areas. The role of the dust in the deliquescence of sea salt is currently under investigation with limited brine. The test setup for CGR needs to be reanalyzed to determine if the specimen has enough constraint for this testing. Further characterization of Teardrop specimens is also underway to identify conditions that favor effective crack growth during testing under natural deliquescence. This characterization includes a more thorough cleaning per ASTM G1 [21], cross sectioning and microscopic analysis of pits and crack fronts. Once the test parameters are optimized, CISCC tests will be run to measure K_{ISCC} on base metal and simulated HAZ specimens to examine the role of stress intensity factors and sensitization of material on CGR in dry salt environments.

ACKNOWLEDGEMENT

This work at the Savannah River National Laboratory was sponsored by the Spent Fuel and Waste and Science

Technology (SFWST) Program, Office of Nuclear Energy under the U.S. Department of Energy, and by the Savannah River Nuclear Solutions, LLC under Contract No. DE-AC09-08SR22470 with the U.S. Department of Energy. The assistance of Kallie Metzger, Kellie Hair, Matt Van Swol, David Missimer and Henry Ajo during the characterization of the specimens is gratefully acknowledged.

REFERENCES

[1] Lam, P.S. and Sindelar, R. L "Flaw Stability Considering Residual Stress for Aging Management of Spent Nuclear Fuel Multiple-Purpose Canisters," Journal of Pressure Vessel Technology, AUGUST 2016, Vol. 138 / 041406-1-11.

[2] Tani, J.I., 2009, "Initiation and Propagation of Stress Corrosion Cracking of Stainless Steel Canister for Concrete Cask Storage of Spent Nuclear Fuel," Corrosion, Vol. 65, No. 3, pp. 187-194.

[3] Caseres, L. and Mintz, T.S., 2010, Atmospheric Stress Corrosion Cracking Susceptibility of Welded and Unwelded 304, 304L, and 316L Austenitic Stainless Steels Commonly Used for Dry Cask Storage Containers Exposed to Marine Environments, NUREG/CR-7030, Office of Nuclear Regulatory Research, U.S. Nuclear Regulatory Commission, Washington, D.C., USA.

[4] Shirai, K., Tani, J. ,and Saegusa, T., 2011, "Study on Interim Storage of Spent Nuclear Fuel by Concrete Cask for Practical Use - Feasibility Study on Prevention of Chloride Induced Stress Corrosion Cracking for Type 304L Stainless Steel Canister," CRIEPI N10035, Central Research Institute of Electric Power Industry, Tokyo, Japan (In Japanese).

[5] He, X., Mintz, T. S., Pabalan, R., Miller, L., and Oberson, G., 2014, Assessment of Stress Corrosion Cracking Susceptibility for Austenitic Stainless Steels Exposed to Atmospheric Chloride and Non-Chloride Salts, NUREG/CR-7170, Office of Nuclear Regulatory Research, U.S. Nuclear Regulatory Commission, Washington, D.C., USA.

[6] Enos, D.G. and Bryan, C.R., *Final Report: Characterization of Canister Mockup Weld Residual Stresses*, FCRD-UFD-2016-00064, Sandia National Laboratories, November, 2016.

[7] D.G. Enos and C.R. Bryan, "Status report: Characterization of Weld Residual Stresses on a Full Diameter SNF Interim Storage Canister Mockup," FCRD-UFD-2015-00123 Sandia National Laboratories, August, 2015

[8] API 579-1/ASME FFS-1, 2007, *Fitness-For-Service* (API 579 Second Edition), American Petroleum Institute, Washington, DC., USA.

[9] *Standard Review Plan for Renewal of Specific Licenses and Certificates of Compliance for Dry Storage of Spent Nuclear Fuel*, NUREG-1927, Rev. 1., Office of Nuclear Material Safety and Safeguards, U.S. Nuclear Regulatory Commission, Washington, D.C., USA, ML15180A011.

[10] ASME Boiler and Pressure Vessel Code, Section XI, *Rules for Inservice Inspection of Nuclear Power Plant Components*, 2013, American Society of Mechanical Engineers, New York, NY., USA.

[11] Chu, S., 2014, *Flaw Growth and Flaw Tolerance Assessment for Dry Cask Storage Canisters*, No. 3002002785, Electric Power Research Institute, Palo Alto, CA., USA.

[12] Broussard, J.E., Limiting Flaw Size Evaluation for Welded Austenitic Stainless Steels: A Comparison of Section XI Appendix C and Appendix H Approaches, Proceedings from the ASME Pressure Vessels and Piping Conference, Vancouver, CA, PVP2016-64037

[13] Shirai, K., Tani, J., Arai, T., Watatu, M., Takeda, H., Saegusa, T., Windton, P.L., 2008, "Research on Spent Fuel Storage and Transportation in CRIEPI (Part 2 Concrete Cask Storage)," Paper ID P16P1215, 16th Pacific Basin Nuclear Conference (16PBNC), Aomori, Japan; Reprinted by Idaho National Laboratory, INL/CON-08-14592, Idaho Falls, ID, U.S.A.

[14] Kosaki, A., (2006), "SCC Propagation Rate of Type 304, 304L Steels Under Oceanic Air Environment," ASME Paper No. ICONE14-89271.

[15] Kosaki, A., 2008, "Evaluation method of corrosion lifetime of conventional stainless steel canister under oceanic air environment," Nuclear Engineering and Design, 238, pp. 1233–1240.

[16] Tani, J., Mayuzumi, M., Arai, T., and Hara, N., 2007, "Stress Corrosion Cracking Growth Rates of Candidate Canister Materials for Spent Nuclear Fuel Storage in Chloride-Containing Atmosphere," Mater. Trans., 48(6), pp. 1431–1437.

[17] Sindelar, R.L., Garcia-Diaz, B. L., Carter, J.T., Lam, P.S., Duncan, A.J., and Wiersma, B. J. "Chloride-Induced Stress Corrosion Crack Growth Under Dry Salt Conditions – Application to Evaluate Growth Rates in Multipurpose Canisters," Proceedings from the ASME Pressure Vessels and Piping Conference, Vancouver, CA, PVP2016-63884

[18] ASTM E1681-03 (2013), "Standard Test Method for Determining Threshold Stress Intensity Factor for Environment-Assisted Cracking of Metallic Materials," ASTM International, West Conshohocken, PA, 2013

[19] ASTM E104 - 02(2012), "Standard Practice for Maintaining Constant Relative Humidity by Means of Aqueous Solutions," ASTM International, West Conshohocken, PA, 2012

[20] Lam, P.S., Zapp, P.E., Duffey, J. M., Dunn, K. A. Stress "Corrosion Cracking In Tear Drop Specimens," Proceedings of the ASME 2009 Pressure Vessels and Piping Division Conference, Prague, Czech 2009, PVP2009-77432

[21] ASTM G1 - 03(2011), "Standard Practice for Preparing, Cleaning, and Evaluating Corrosion Test Specimens," ASTM International, West Conshohocken, PA, 2011